Path Planning and Obstacle Avoidance for Mobile Manipulator Robots

Yuwei Pan *

School of Advanced Technology, Xi'an Jiaotong-Liverpool University, Suzhou, China

* Corresponding Author Email: Yuwei.Pan24@student.xjtlu.edu.cn

Abstract. Mobile manipulator robots have been instrumental in a number of industries and have been applied in manufacturing, logistics, energy, and medicine, especially during this period of rapid technological development worldwide. They can also address a variety of challenges that arise from keeping up with the times. However, mobile manipulator robots frequently struggle with insufficient positioning ability, inadequate computational efficiency, and difficulty functioning effectively in dynamic and shifting circumstances where path planning is disrupted by external factors. Regarding the aforementioned issues, this article will discuss four strategies to enhance the balance between robotic arms and AMR as well as the mobile manipulator robot's capacity to avoid obstacles. For ongoing development, better coordination between robotic and AMR platforms can result in higher working efficiency for specific tasks, which can raise industries' output capacities. At the same time, the development of mobile manipulator robots might alleviate the strain caused by the decrease in the labor force across many industries. Finally, there is a growing trend that mobile manipulator robots can solve complicated tasks, promoting the diversity of industrialized robots and providing convenience for people's lives.

Keywords: Mobile manipulator robots, Path planning, Obstacle avoidance, Coordination efficiency.

1. Introduction

Mobile robots are able to carry out certain tasks in expansive environments due to their flexibility [1]. Mobile manipulators may use their gripping skills to pick up and place objects [2]. Mobile manipulators have a wide range of applications. They can perform essential tasks in factories [3], transport coffee indoors and outdoors [4], and explore outer space [5]. Kuka has begun using the KMR iisy robot in industries to perform tasks such as raw material delivery, sorting, and stocking. Hikvision robots can assist with transportation in medical settings. SONY, in partnership with several companies and universities, developed the LEV-2 lunar variable robot, which was later used for lunar exploration. Moreover, the development of robots can effectively counteract the decline in the future labor force, and their ability to operate 24 hours a day can significantly improve production and transportation efficiency to adapt to future challenges.

For the VIEF method, previous studies mainly fall into three categories. Method one involves separating the system and planning and controlling the robotic arm and the mobile operating robot separately [6]. For instance, the A algorithm is used to plan the mobile chassis, and the RRT algorithm is used to plan the robotic arm, which reduces the system's utilization rate. Method two regards the system as a high-degree-of-freedom robot [7, 8]. However, its computational cost is often high, which is not conducive to application. Method three uses a hierarchical optimizer such as HAMP and takes into account the system characteristics to optimize the separation system method. Regarding the Dynamic Window Approach, the original DWA method, while planning the course, assumes that the robot's speed is constant and can only generate straight lines and arcs [9]. Similar to the Speed Obstacle Method (VO), it cannot effectively assist the robot in avoiding obstacles in complex situations. For the third approach, Sampling-with-Path based Planning, the conventional path planner (RRT, PRM) is limited to offering one obstacle avoidance path, and the calculation time is rather long when dealing with restricted settings. As a result, it cannot be employed for the real-time obstacle avoidance path of non-holonomic robots.

However, the three methods introduced next in this article will effectively assist in planning the path. Method one (VIEF): This method can be applied to robots with non-holonomic constraints, and it introduces a cost function that not only improves obstacle avoidance efficiency but also enhances the synergy between the robotic arm and the mobile robot, maintains the tracking accuracy of the end effector, and ensures a smooth path with a short response time [9]. Method two (DWV): This method is an upgrade of the DWA approach, capable of generating more complex paths to achieve flexible obstacle avoidance and enhancing the feasibility of the paths. As it is an improvement based on DWA, this method can be practically applied to robots [10]. Method three (Sampling-with-Path based Planning): This method has developed the RRT-Flex planner, successfully reducing the rejection rate of path sampling, improving the connectivity of various states of the robot, and enhancing the quality of the path. Moreover, this method is developed based on the traditional RRT planner and can be practically applied [11].

2. Methods

2.1. Create virtual impedance energy field to constrain the movement (VIEF)

The whole system achieves balance through the mobile robot, the robot arm, and the end effector. By creating a virtual impedance between the constraint position and the end effector, this technique indirectly adjusts the force. The whole system is based on Mass-damper-spring system, which is shown as follows.

$$Z(s) = \frac{F(s)}{\dot{x}(s)} = Ms + B + \frac{K}{s} \tag{1}$$

$$M_d \Delta\ddot{p} + B_d \Delta p + K_d \Delta p = F(\Delta p = p_d - p) \tag{2}$$

where M_d is desired mass. K_d is spring constant. $B_d$is damping constant. Δp defines error. p_d is equilibrium position.

This method mainly focuses on mechanical impedance. Fig. 1 and equation (1) demonstrate the relationship between external force *F*, mass *M*, damping constant *B*, and spring constant *K*. When an external force acts on the whole system, the position deviation (Δp) can produce an elastic force (K_d Δp), a damping force (B_dΔṗ), and an inertial force (M_dΔp̈), which drive the system from the current position toward the ideal position.

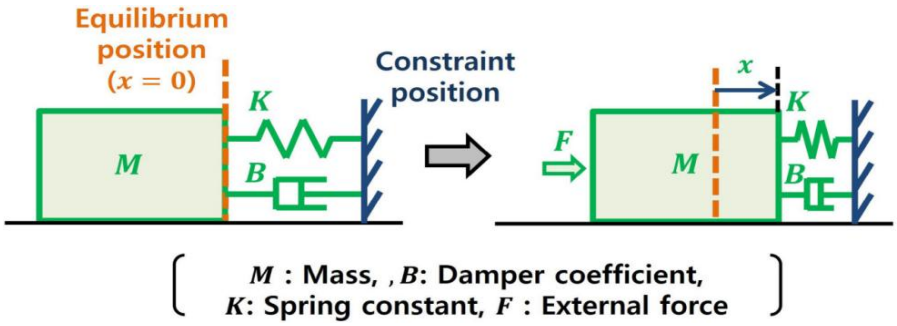

Fig. 1 Mass-damper-spring system

As shown in Fig. 2, an error Δp is created between the current position *p* and the equilibrium position p_d of the manipulator's end effector when the user adjusts it to the desired position. The virtual impedance from equation (3), an error equation, can be used to control the end effector. To adjust the motion characteristics of the end effector, the user may modify the desired mass M_d, spring constant K_d, and damping constant B_d for each axis. In this study, virtual impedance is employed to help a mobile robot successfully follow the trajectory of the end effector. This VIEF approach enables the mobile robot to track the end effector. As shown in Fig. 3, the system applies DWA for the path planning of the mobile robot, which consists of four steps and is shown as follows.

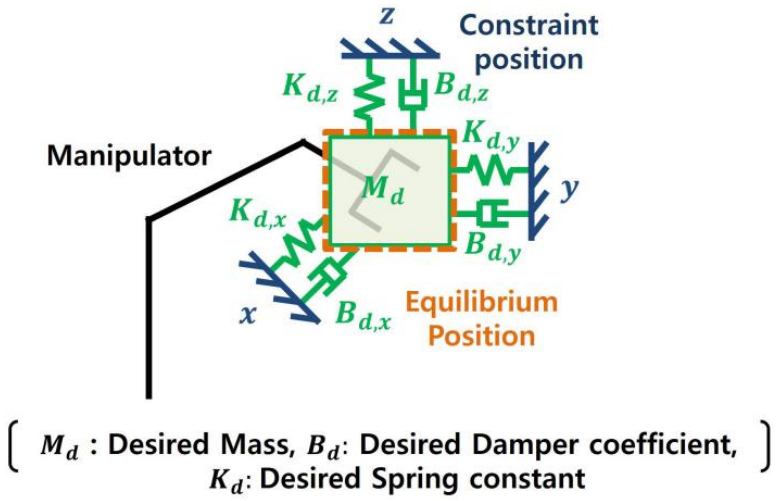

Fig. 2 Impedance control of manipulators

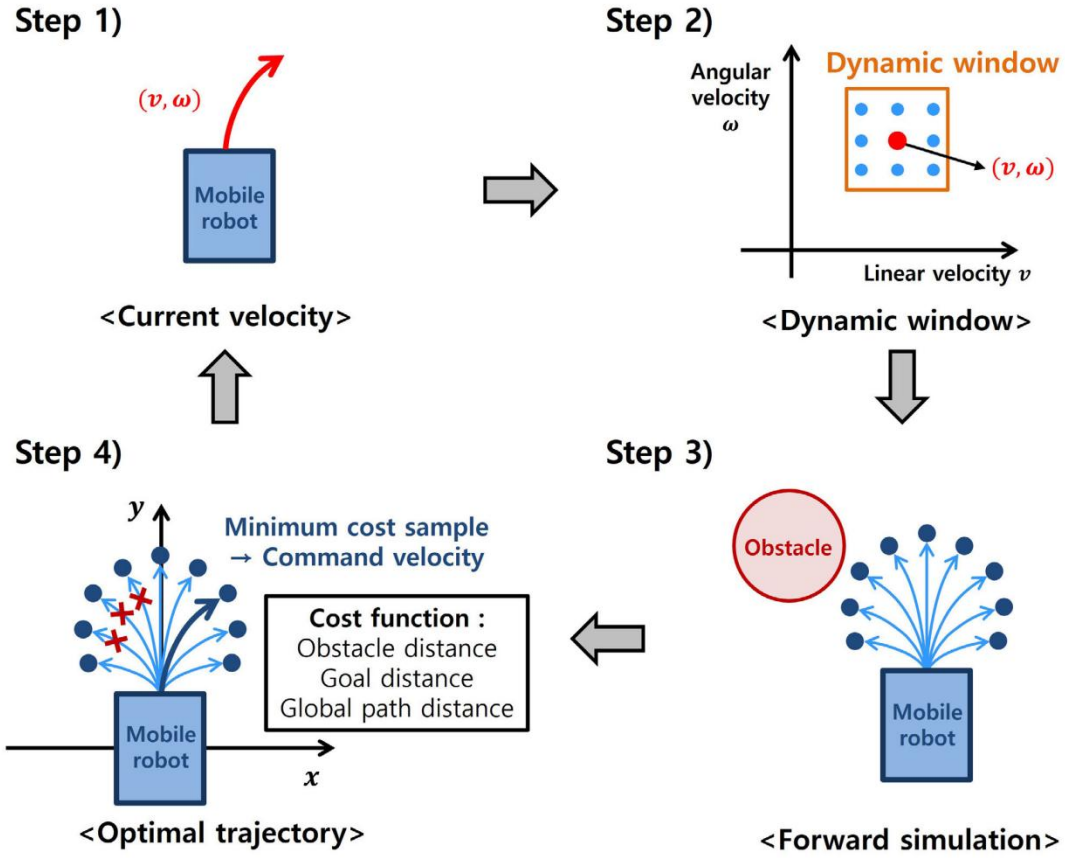

Fig. 3 DWA algorithm

In the first step, the current linear velocity (*V*) and angular velocity (ω) of the mobile robot are measured. The second step involves creating a velocity boundary in the velocity space centered on the current linear and angular velocities, which is referred to as the dynamic window. In the third step, the trajectory is obtained through forward simulation generated from a given velocity. In the fourth step, the total cost of each trajectory is calculated using several cost functions, and the trajectory with the lowest energy consumption is selected as the optimal one. The corresponding velocity is then output as the next commanded velocity. This four-step cycle continues until the optimal velocity is found under dynamic changes. In conclusion, the virtual impedance energy field provides the mobile robot with a resistive force, establishing a relationship of mutual restriction and allowing the mobile manipulator to make real-time adjustments.

2.2. DMV

DMV is a system that combines virtual robotic arms (VM) with traditional DMA technology to enable obstacle avoidance in dynamic, narrow environments containing obstacles. The model used in this experiment is a mobile wheeled robot with both a local coordinate system (∑LC) and a global coordinate system (∑GB). With the origin at the robot's starting position and denoted by the superscript GB, the global coordinate system is used to represent the robot's location within the wider environment. With the origin at the center of the two wheels and without the superscript GB, the local coordinate system is used to describe the robot's relative motion.

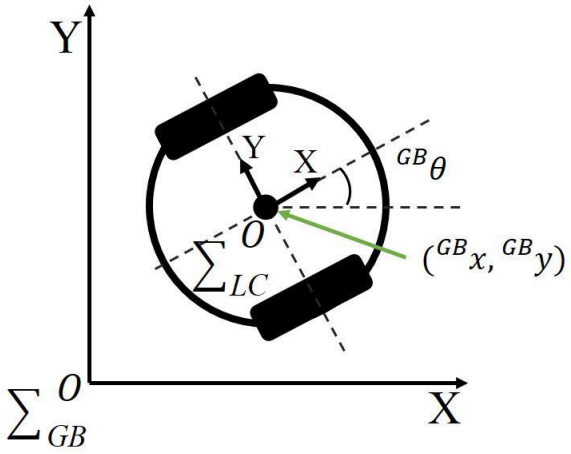

Fig. 4 Coordinate system of mobile robot

The robot's position and orientation in the global coordinate system are represented by the angles GB_θ and the coordinatesGB_x and GB_y, as shown in Fig. 4. The relevant speed derivations are as follows.

$$GB_{\dot{\theta}}=\omega \tag{3}$$

$$GB_{\dot{x}}=v\cos GB_\theta \tag{4}$$

$$GB_{\dot{y}}=v\sin GB_\theta \tag{5}$$

$$GB_\theta=\int_0^t \omega dt\, dt\mathrm{w} \tag{6}$$

Where V is translational velocity and ω is angular velocity.

2.2.1. Dynamic window approach (DWA)

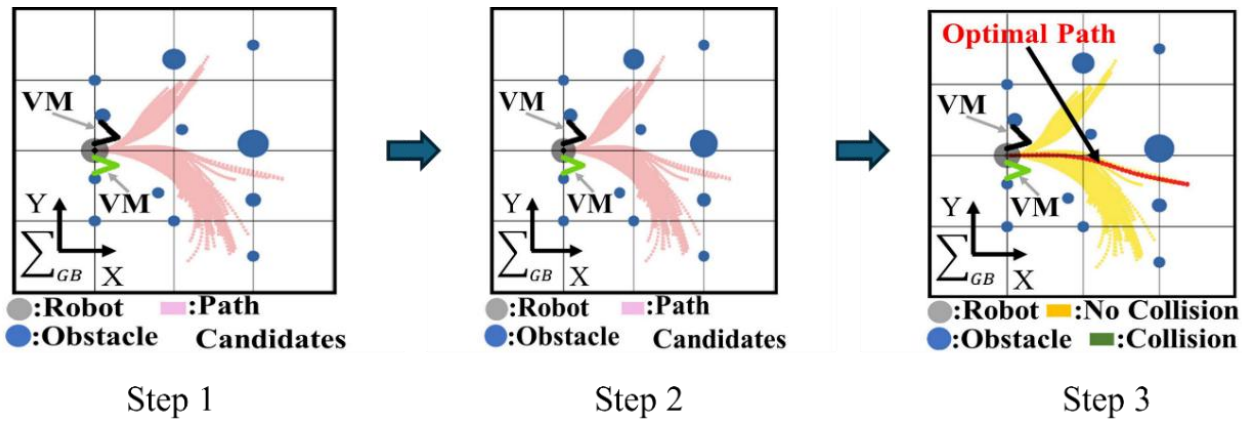

Fig. 5 Three steps of DWA

DWA is a technique for local path control of robots, which consists of three steps, as shown in Fig. 5. Step one: Based on the robot's speed and associated characteristics, generate the appropriate velocity space (VSD) under dynamic constraints; Step two: Generate candidate paths from the velocity samples in the VSD; Step three: Construct the cost function, evaluate the candidate paths, and determine the optimal path.

2.2.2. Virtual manipulators

The virtual manipulator consists of a virtual leader manipulator and a virtual assistant manipulator. The former is responsible for path tracking, while the latter handles obstacle avoidance tasks. The concept of virtual mechanical hands is illustrated in Fig. 6.

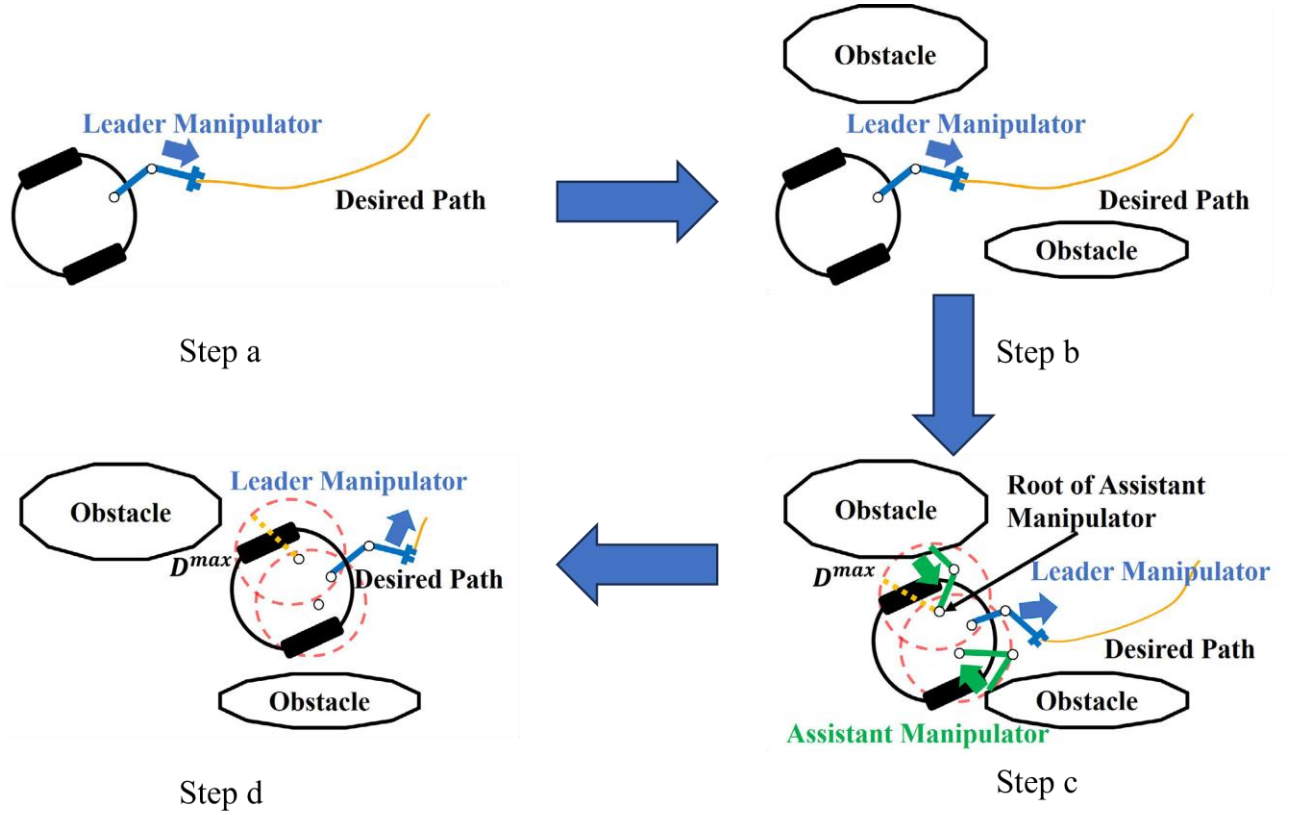

Fig. 6 Four steps of virtual manipulator

Obstacle avoidance is executed conditionally. The wheeled robot is equipped with a lidar that measures the distance between the root of the virtual assistant manipulator and the obstacle. The virtual assistant manipulator will not respond if the distance D exceeds the threshold D^{MAX}. However, when the distance falls below the threshold D^{MAX}, the virtual assistant manipulator will initiate obstacle avoidance behavior. The following presents the calculation of reflexive motion using a virtual two-link manipulator.

$$\dot{q}=J^{\#}\dot{x}+\lambda(I-J^{\#}J)(\Theta_{nj}^{ref}-\theta_{nj}^{res}) \tag{7}$$

Where $\dot{q}$: state error; $J^{\#}$: pseudo-inverse Jacobian matrix; λ: weight coefficients of the null-space; Θ_{nj}^{ref}: reference angle of the virtual manipulator; θ_{nj}^{res}: response angle of the virtual manipulator

Virtual manipulators and DMA technology work together to calculate and generate the optimal path on roadways containing both static and dynamic obstacles. The DMA determines the fundamental angular velocity, while the virtual manipulator determines the additional angular velocity required for obstacle avoidance. Candidate paths are then generated, cost functions are applied, and the optimal path is ultimately selected.

Step one: Obtain the initial speed through DMA and generate the traditional arc-shaped path; Step two: Perform obstacle avoidance through the VM. The VM intervenes and calculates the velocity required for current obstacle avoidance, ensuring that the path avoids obstacles; Step three: Generate the first output velocity through DWA and the VM in step one. Based on this output velocity, superimpose the velocity required for obstacle avoidance calculated by the current VM; Step four: Repeat the above process until the final obstacle-avoidance path and complete trajectory are generated. The details are illustrated in Fig. 7.

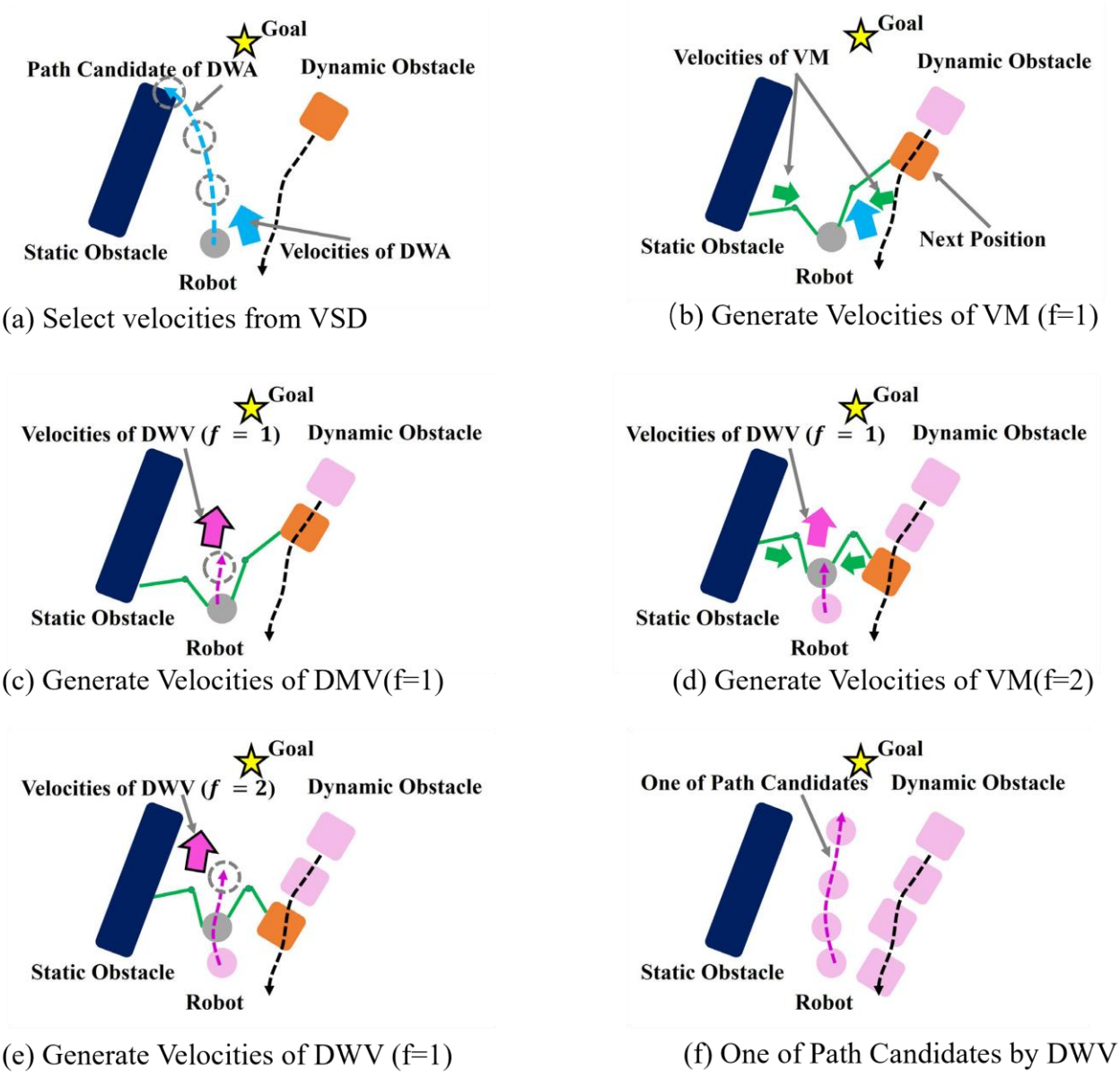

Fig. 7 Concept of DWV

The *f*-th velocities of DWV are calculated as follows.

$$v^{dwv}=v^{dwa} \tag{8}$$

$$w_f^{dwv}=\begin{cases} w^{dwa}+w_f^{vm}, \text{if } f=1 \\ w_{f-1}^{dwv}+w_f^{vm}, \text{otherwise} \end{cases} \tag{9}$$

where v^{dwv} and w_f^{dwv} mean translational and the angular velocities of DWV.

Lastly, cost functions are constructed in order to assess the robot‘s optimal paths.

2.3. Sampling-with-path based planning

The parallel mechanism motion planning problem, shown in Fig. 8, is a common non-holonomic motion planning example to demonstrate this concept.

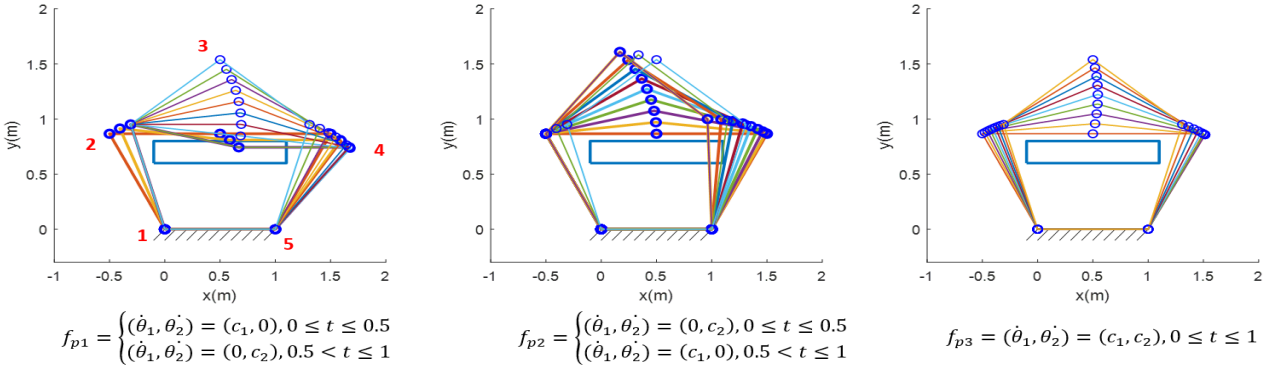

Fig. 8 Parallel Mechanism motion planning with protocol function set

To overcome the drawbacks of conventional path planning techniques (RRT, RRT-Connect, PRM), including the inability to rapidly plan high-quality paths and to meet the requirements of robots with non-holonomic constraints. This method primarily employs connection function sets and integrates the RRT-Flex planner within the RRT-Connect framework. Ultimately, the planner (Find Valid Connection function) selects effective pathways, thereby improving the path-planning efficiency and obstacle-avoidance success rate of mobile robots with mechanical arms.

First, the sampling method is chosen as neighborhood sampling to prevent sampled points from reaching distant locations, reduce unnecessary sampling, and match newly sampled states with existing states in the tree to form adjacent state pairs. A two-dimensional planar motion space and a collection of protocol functions with parameters such as joint angles and time *t* are used in this figure to illustrate motion planning for a parallel mechanism. This serves as an explanation of imperfect motion planning and reflects the sampled states and neighboring state pairings. Then, multiple paths are generated using connection function sets. Third, the FindValidConnection function is applied to filter valid paths that can avoid obstacles. The detail functions can be descrbied as follows:

$$f_{pi}(q_s,q_g,\theta_s,t)=\begin{cases} f_{pi}(q_s,\theta_s,t),0\le t\le t_s \\ f_{pi}(q_s,\theta_s,t),t_s\le t\le 1\text{-}t_e \\ f_{pi}(q_g,\theta_s,t),1\text{-}t_e\le t\le 1 \end{cases} \tag{10}$$

where q_s: start state q_g:goal state θ_s:Parameters related to the system's pose and direction; t: Time parameter; t_s=The threshold for the end time of the initial transition interval; t_e=The starting time threshold of the final transition interval.

Finally, to continuously improve the route, the RRT-Flex planner eliminates unnecessary sample points, re-interpolates the remaining paths, and iteratively refines them by considering the total path length and curvature.

3. Results and Discussion

3.1. Result one of VIEF

Experiments were conducted using the ROS framework and the Gazebo simulation environment. The software and hardware configurations are as follows. Cartesian space PD control was implemented on a Scout 2.0 differential drive robot, a Panda robotic arm with seven degrees of freedom, a 3D LiDAR (VLP-6) sensor, and the *franka_ros* package. Mobile robot planning: Based on the navigation and *move_base_flex* packages, a custom DWA algorithm module was created, with VIEF and obstacle fields used as cost maps.

Trajectory generation: The trajectory of the end effector was planned to use the linear segment plus parabolic blend (LSPB) approach.

Simulation 1 analyzed the robot's ability to avoid obstacles along a linear trajectory with cylindrical obstacles, as well as the tracking stability of the end effector.

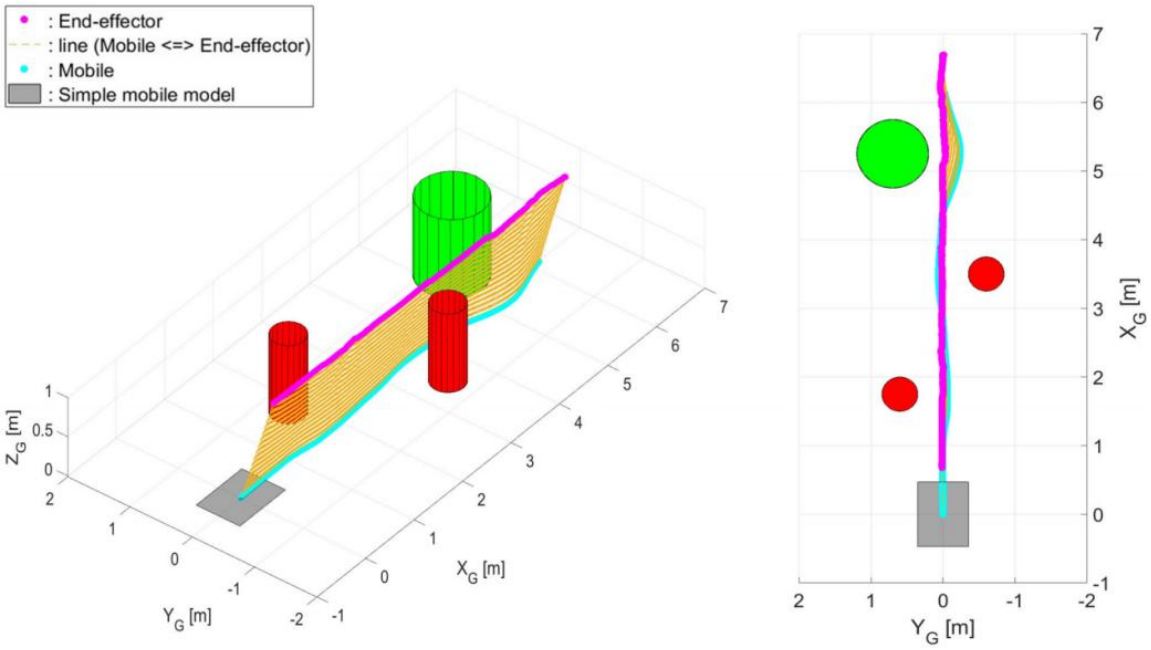

Fig. 9 Pose graph

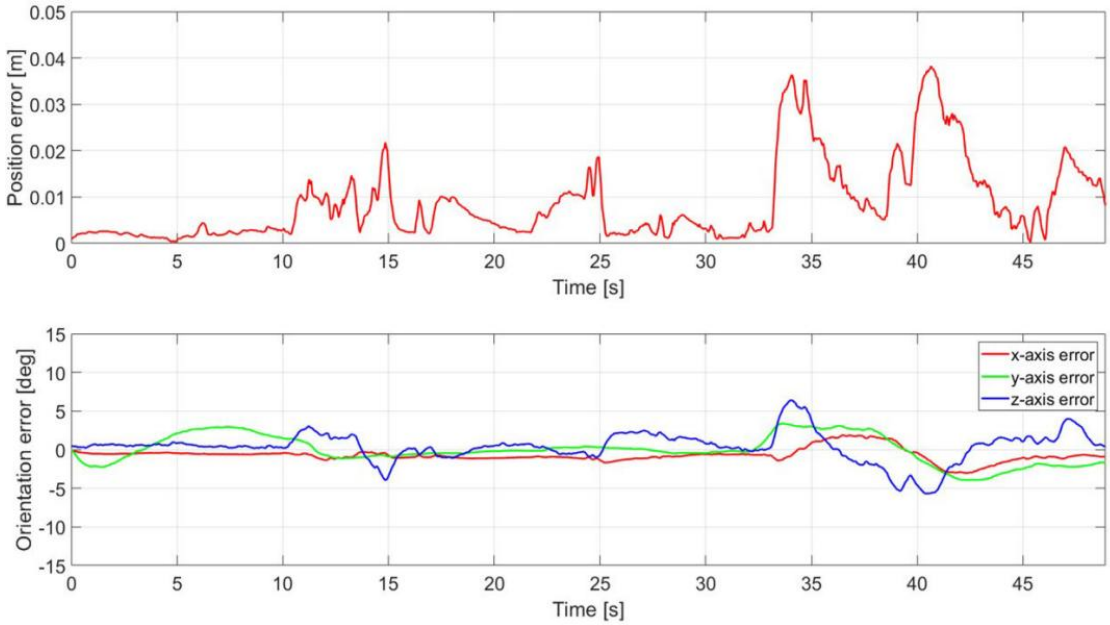

Fig. 10 Pose error of end-effector

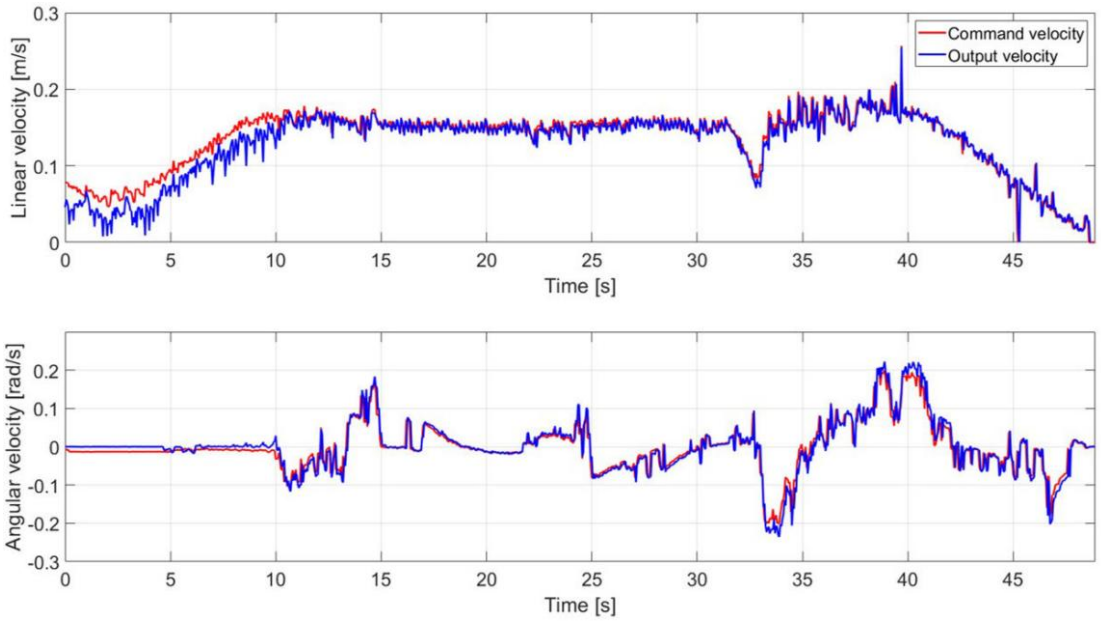

Fig. 11 Mobile robot commanded and output velocity

The above three pictures (Fig. 9, Fig. 10, Fig. 11) respectively describe pose graph, pose error of end-effector. Mobile robot commanded and output velocity.

During the obstacle-avoidance process, the mobile robot successfully avoided all obstacles, and the end effector followed the ideal trajectory with a maximum error of 0.0383 m and an average position error of 0.00864 m. Furthermore, the mobile robot's motion trajectory was S-shaped, with alternating positive and negative angular velocities, while the linear velocity was nearly equal to the set speed of the end effector. The robot and the manipulator maintained an optimal distance, indicating greater synchronization and improved obstacle-avoidance capability.

This method has the advantage of subjecting the mobile robot to an impedance force by establishing a virtual impedance connection and applying a cost function. This enables the mobile robot to follow the trajectory of the end effector, improving overall obstacle-avoidance performance in specific tasks and producing smoother motion. It also mitigates some drawbacks of non-holonomic robots. However, certain limitations exist. In deriving the corresponding formulas, p is assumed to be zero and the robot is considered to have inertia, which may lead to an imprecise impedance relationship between the manipulator and the mobile robot. In addition, the influence of the ratio of the spring constant to the damping constant on the experiment is not taken into account.

3.2. Result one of DMV

As shown in Fig. 12, a total of four cases were designed and shown above for simulation experiments:

Case One: Ten static obstacles were randomly placed in the simulation environment.

Case Two: Ten dynamic obstacles were randomly placed in the simulation environment. The green obstacle moved at a speed of 0.3 m/s, while the pink obstacle moved at a speed of 0.25 m/s.

Case Three: Thirty static and dynamic obstacles were randomly placed in the simulation environment. The obstacle speed range was randomly set between 0.0 m/s and 0.2 m/s, not exceeding the maximum speed of the robot.

Case Four: The conditions were the same as in Case Three, but the random obstacle speed range was extended to 0.0 m/s–0.6 m/s, with some obstacles assigned speeds exceeding the maximum speed of the robot.

Finally, the wheeled robots using SLP, DMA, and DWV technologies, respectively, were tested in these four environments

The success rates of robots using DWV technology in Cases One, Two, Three, and Four were 100%, 100%, 85%, and 70%, respectively; The success rates of robots using DWA technology were

100%, 0%, 32%, and 4%, respectively; The success rates of robots using SLP technology were 100%, 0%, 14%, and 6%, respectively.

The benefits of DMV include enabling robots to plan optimal paths more effectively and flexibly avoid obstacles in environments with dynamic impediments. However, DMV also has drawbacks: parameter computation is relatively complex, requiring extensive modeling and testing before practical implementation, and the method tends to become trapped in local path optimization at the expense of global optimality.

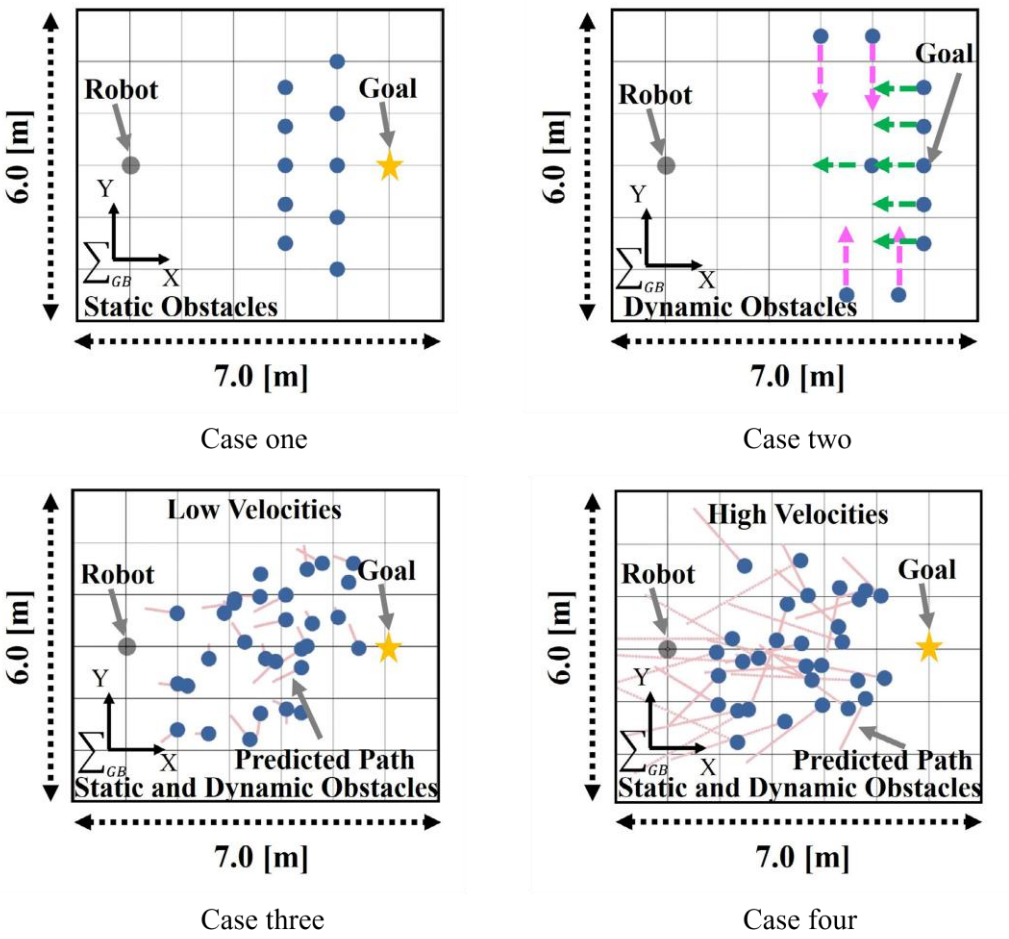

Fig. 12 Four cases of the simulation

3.3. Result of sampling-with-path

The experiment was conducted using MoveIt!. The platform is based on the Clearpath Husky wheeled mobile chassis equipped with a UR5e robotic arm, which has six degrees of freedom and employs four planners (RRT-Flex, RRTC, PRM, and RRT). The end effector of the robot carried a load measuring 0.6 m × 0.5 m × 0.1 m. The simulation environment included barriers such as doors and boxes.

As shown in Fig. 13, the simulation included five scenes:

Scene 1: From the starting position to the target position, a 1.2 m × 2 m door had to be bypassed, with the starting point located close to the door.

Scene 2: Similar to Scene 1, but the starting point was shifted away from the door and closer to the wall, making path planning more difficult.

Scene 3: Two box obstacles were placed in the environment, and a path had to be planned from the starting position to the target position.

Scene 4: Building on Scene 3, a third box obstacle was added to further block the direct path.

Scene 5: Two 1.7 m × 2 m doors (with lateral offset settings) had to be bypassed from the starting position to the target position.

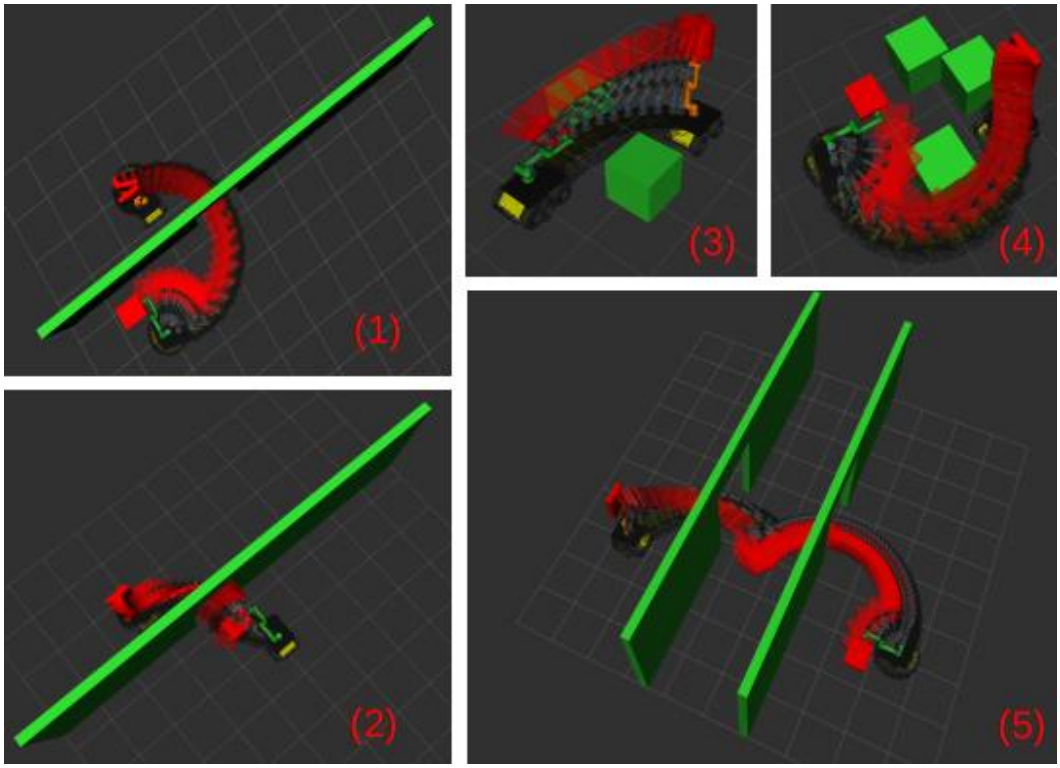

Fig. 13 Environment settings for five planning scenarios

The experimental results are shown in Fig. 14.

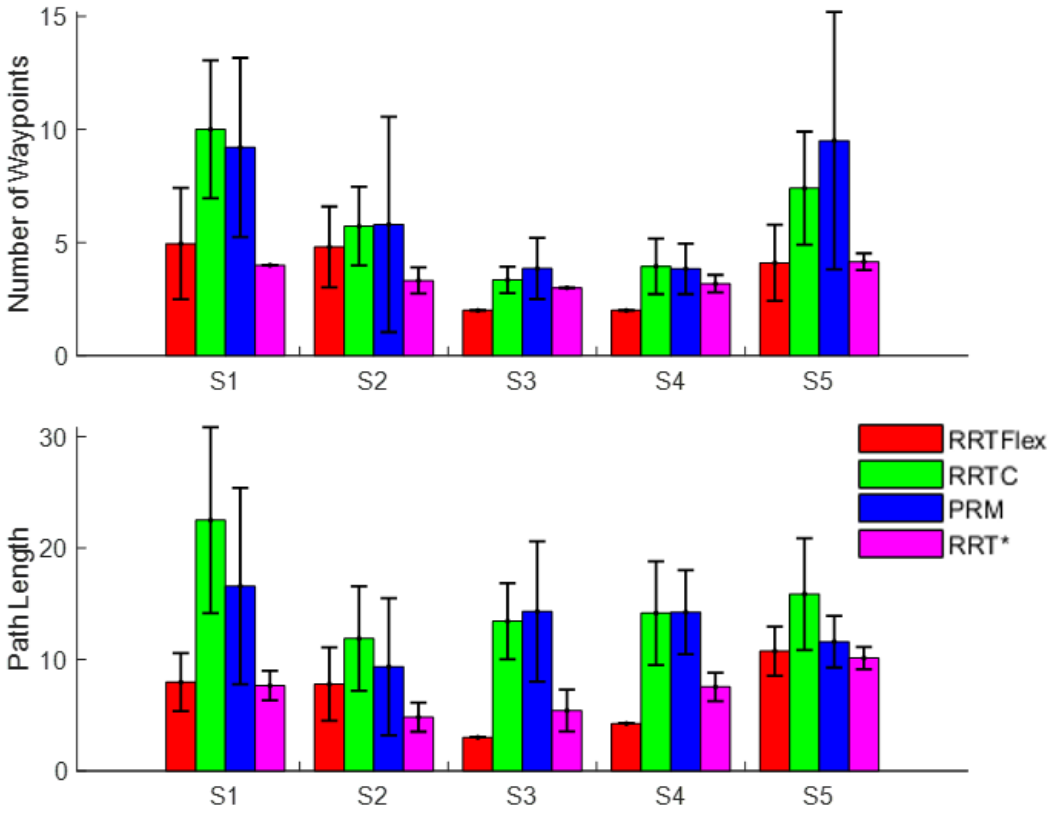

Fig. 14 Planning results comparison between planners

Fig. 14 demonstrates the results of the simulation. Robots using the RRT-Flex planner achieved the highest obstacle-avoidance success rate across various scenarios. In addition, the number of path points was significantly reduced in all cases, and the overall path length was generally shorter.

4. Conclusion

The VIEF method can significantly enhance the obstacle-avoidance path-planning capability of mobile manipulator robots, improve coordination between mobile robots and mechanical arms, and enable them to perform tasks in more complex environments, such as factories, logistics companies, and pharmaceutical companies, thereby increasing industrial production efficiency. However, since this method does not take robot inertia into account, its mathematical characteristics and optimization can be further refined in future studies. The DWV method can effectively help mobile manipulator robots avoid static and dynamic obstacles in real time. It is suitable for applications in environments such as hospitals or homes where people are moving around. Nevertheless, this method also has drawbacks, such as not considering obstacles with sudden speed changes and the possibility of becoming trapped in a locally optimal path. In the future, global path planners can be introduced, and studies can be conducted on strategies to avoid objects with sudden velocity variations. Finally, the sampling-with-path-based planning method can explore diverse paths in complex environments. It has potential applications in autonomous driving technology; however, since it does not consider the maximum acceleration constraints of robots or the degrees of freedom of joints, future improvements could incorporate constraint-handling techniques to further optimize the algorithm.

References

[1] Nehmzow, U. (2001). Mobile robotics: Research, applications and challenges. Proceedings of the Institution of Mechanical Engineers, London, U.K., pp. 1–4.

[2] Ali, M. H., Aizat, K., Yerkhan, K., Zhandos, T., and Anuar, O. (2018). Vision-based robot manipulator for industrial applications. Procedia Computer Science, 133, 205–212.

[3] Outón, J. L., Villaverde, I., Herrero, H., Esnaola, U., and Sierra, B. (2019). Innovative mobile manipulator solution for modern flexible manufacturing processes. Sensors, 19 (24), 5414.

[4] Pratkanis, A., Leeper, A. E., and Salisbury, K. (2013). Replacing the office intern: An autonomous coffee run with a mobile manipulator. Proceedings of the IEEE International Conference on Robotics and Automation, Karlsruhe, Germany, May, pp. 1248–1253.

[5] Li, Z., Moran, P., Dong, Q., Shaw, R. J., and Hauser, K. (2017). Development of a tele-nursing mobile manipulator for remote care-giving in quarantine areas. Proceedings of the IEEE International Conference on Robotics and Automation (ICRA), May, pp. 3581–3586.

[6] Rastegarpanah, A., Gonzalez, H. C., and Stolkin, R. (2021). Semi-autonomous behaviour tree-based framework for sorting electric vehicle batteries components. Robotics, 10 (2), 82.

[7] Shao, J., Xiong, H., Liao, J., Song, W., Chen, Z., Gu, J., and Zhu, S. (2021). RRT-GoalBias and path smoothing based motion planning of mobile manipulators with obstacle avoidance. Proceedings of the IEEE International Conference on Real-time Computing and Robotics (RCAR), Xining, China, July, pp. 217–222.

[8] Wang, C., Zhang, Q., Tian, Q., Li, S., Wang, X., Lane, D., Petillot, Y., and Wang, S. (2020). Learning mobile manipulation through deep reinforcement learning. Sensors, 20 (3), 939.

[9] Choi, J. H., Sagong, U. H., Park, J. H., Kim, M., and Hwang, M. J. (2024). Motion planning of mobile manipulator using virtual impedance energy field. IEEE Access, 12, 89776–89793.

[10] Kobayashi, M., and Motoi, N. (2022). Local path planning: Dynamic window approach with virtual manipulators considering dynamic obstacles. IEEE Access, 10, 17018–17029.

[11] Yuan, Q. (2024). Sampling-with-path based planning: Easing non-holonomic mobile manipulator motion planning. Proceedings of the 9th International Conference on Robotics and Automation Engineering (ICRAE), Singapore, pp. 188–192.